

Risk-aware Selective Prompting for Hallucination Mitigation in Large Vision-Language Models

Yuang Huang¹ and YaFeng Zhang² and Zilan Yu³

¹Shanghai Jiao Tong University ²iFLYTEK ³Tsinghua University
yuang.huang@sjtu.edu.cn yfzhang40@iflytek.com yuz122@mails.tsinghua.edu.cn

Abstract

Prompt-based verification is widely used to mitigate hallucinations in large vision-language models (LVLMs), yet when it helps remains poorly understood. We systematically study verification prompting across two representative LVLM architectures and hallucination benchmarks, and find that it is a *risk-bearing intervention*: its corrections increase with input difficulty, while newly introduced errors persist across difficulty levels. As a result, always-on prompting helps on hard inputs but offers little benefit—and can harm—easier ones. Our analysis further shows that this behavior is associated with a conservative output shift. Verification prompts redistribute attention from visual tokens toward instruction tokens and induce a distinct middle-layer entropy pattern absent in a neutral-prompt control, suggesting instruction-conditioned attention redistribution rather than uniformly improved visual grounding. Motivated by this input-dependent risk, we propose Risk-aware Selective Prompting (RSP), a training-free approach that uses pre-generation uncertainty signals to trigger verification selectively. RSP mitigates the degradation of always-on prompting while preserving baseline performance, and reveals that effective selection signals vary across architectures.

1 Introduction

Large vision-language models (LVLMs) such as LLaVA (Liu et al., 2023), InstructBLIP (Dai et al., 2023), and GPT-4V (OpenAI, 2023) have achieved remarkable performance on visual understanding tasks, yet they frequently generate descriptions of objects absent from the image—a phenomenon known as *object hallucination* (Li et al., 2023; Rohrbach et al., 2018). Among mitigation strategies, prompt-based verification, such as instructing the model to check visual evidence or answer more carefully, is attractive because it requires no retraining or architectural modification.

In current practice, such verification prompts are often applied indiscriminately to all inputs (always-on prompting). However, this raises a question that has received little systematic attention: **does verification prompting always help, or can it sometimes cause harm?** We argue that verification prompting should be viewed not as a universally beneficial add-on, but as a risk-bearing intervention that should be applied selectively depending on the input. Recent work has shown that chain-of-thought prompting can reduce performance on certain tasks (Sprague et al., 2024), but when such harm occurs in LVLMs, why it occurs, and how to avoid it remain underexplored.

We investigate this question empirically through evaluation on POPE across two architecturally distinct LVLMs. Our analysis reveals three findings.

It introduces a relatively stable number of new errors (*breaks*) across difficulty levels, while the number of errors it corrects (*fixes*) increases with difficulty. On easy inputs, fixes and breaks nearly cancel; on hard inputs, fixes far exceed breaks. This asymmetry explains why always-on prompting helps on adversarial inputs but provides little benefit and can harm easier ones.

By probing attention maps across transformer layers under verification, neutral, and no-prompt conditions, we find that verification prompts draw attention toward instruction tokens, reduce relative attention to visual tokens, and induce a distinct middle-layer entropy pattern not reproduced by a neutral-prompt control. These observations suggest that verification prompting is associated with instruction-conditioned attention redistribution, rather than clearly indicating uniformly improved visual grounding.

Because prompting is beneficial only for a subset of inputs, we examine whether internal model states before generation can guide the decision to prompt. We find that useful signals appear architecture-sensitive: middle-layer attention en-

tropy is informative for LLaVA-1.5, where visual tokens are directly exposed to the language model, while output-logit confidence is more reliable for InstructBLIP, where visual information is compressed by a Q-Former.

Based on these findings, we propose **Risk-aware Selective Prompting (RSP)**, a training-free strategy that triggers verification only when a pre-generation uncertainty signal indicates high risk. RSP invokes prompting on only a small fraction of inputs, mitigates the degradation of always-on prompting on easier inputs, and remains close to or above baseline performance across our discriminative evaluation.

The contributions of this work are summarized as follows:

(1) We identify verification prompting in LVLMs as an input-dependent, risk-bearing intervention: corrected errors increase with input difficulty, while newly introduced errors remain relatively stable across difficulty levels.

(2) Through layer-wise attention analysis, we show that this conservative output shift is accompanied by attention redistribution from visual tokens toward instruction tokens and a distinct middle-layer entropy pattern absent in a neutral-prompt control.

(3) Motivated by these findings, we propose RSP, a training-free selective prompting strategy that uses pre-generation uncertainty signals to trigger verification on inputs identified as high-risk. We further show that effective routing signals vary across the two architectures we study.

2 Related Work

2.1 Object Hallucination in LVLMs

LVLMs often mention objects that are absent from the image, even when they produce otherwise fluent and plausible responses. This object hallucination problem is commonly studied with CHAIR (Rohrbach et al., 2018), which measures hallucinated object mentions in open-ended captions, and POPE (Li et al., 2023), which casts hallucination detection as yes/no object-presence questions under different difficulty settings. Existing studies link these errors to object co-occurrence priors (Li et al., 2023), weak visual grounding (Zhou et al., 2024), and attention patterns that rely too heavily on textual context instead of image tokens (Huang et al., 2024). These findings motivate grounding-oriented interventions, but leave open *when* such interventions should be applied.

2.2 Hallucination Mitigation Approaches

To mitigate object hallucination, prior work has explored interventions at different stages of the generation pipeline. *Inference-time* methods intervene during decoding or internal representation processing, including attention-based penalties (Huang et al., 2024), contrastive decoding (Leng et al., 2024; Chuang et al., 2024), self-correction feedback, attention-head masking, and activation-space projection (Zhang et al., 2025; Deng and Yang, 2025; Yang et al., 2025; Wan et al., 2025). These methods are often effective but typically require modified decoding procedures or per-token intervention during generation.

Post-hoc methods verify or revise outputs after generation. Examples include Woodpecker (Yin et al., 2024) and Self-Refine (Madaan et al., 2023), which add checking or refinement stages at inference time.

Prompt-based methods offer a lighter alternative. They modify the input instruction, for example by asking the model to verify its own response (Dhuliawala et al., 2023) or to ground answers in visual descriptions before decoding (Sreyan et al., 2025). These methods aim to reduce hallucination without changing the model or decoding procedure. However, prior evaluations of prompt-based mitigation are largely aggregate, offering limited analysis of which inputs benefit, which are harmed, and whether such interventions should be applied uniformly. This leaves open whether verification prompts should be treated as universally beneficial aids or as interventions with input-dependent risk. Our work is complementary to existing mitigation mechanisms: rather than designing another intervention, we study *when* prompt-based verification should be applied and show that internal uncertainty signals enable risk-aware selective prompting. Our goal is therefore not to outperform specialized mitigation systems, but to characterize verification prompting as a selective intervention problem.

2.3 Uncertainty Estimation and Internal Signals

Uncertainty estimation in large language models has been studied using output-based signals such as predictive entropy, semantic entropy, and sampling-based agreement (Kuhn et al., 2023; Kossen et al., 2024; Nikitin et al., 2024). These approaches typically operate during or after generation, relying on token-level probabilities, multiple samples, or com-

pleted outputs. A complementary line of work examines internal model states directly: probing and intervention studies find that specific layers often play an important role in distinguishing or mitigating hallucinated outputs (Chen et al., 2024; Ji et al., 2024; Kim et al., 2025), while layer-wise attention analyses show that visual-token attention varies substantially across depth (Zhang et al., 2024).

To our knowledge, these signals have not been systematically studied as *pre-generation* criteria for prompt-level selective intervention in LVLMs. Relatedly, recent work uses uncertainty for *routing* between different models or inference strategies (Chuang et al., 2025), but operates at the model-selection level. In contrast, we study prompt-level selective intervention within a single LVLM. Importantly, we find that the effective pre-generation signal appears *architecture-sensitive*: internal attention entropy is effective for models with direct image-token input (LLaVA-1.5), while output-logit confidence is more predictive for architectures with intermediate compression modules (InstructBLIP’s Q-Former), where compressed query tokens make attention-based signals less informative in our experiments. This highlights the need for architecture-aware signal selection.

3 Method

We decompose verification prompting into three analytical layers: (1) characterizing its behavioral effect, (2) probing its internal mechanism, and (3) designing a selective triggering strategy.

3.1 Verification Prompting as a Risk-Bearing Intervention

Given an LVLM \mathcal{M} and an input $(x_{\text{img}}, x_{\text{q}})$, let $y_b = \mathcal{M}(x_{\text{img}}, x_{\text{q}})$ denote the baseline response and $y_p = \mathcal{M}(x_{\text{img}}, [s; x_{\text{q}}])$ denote the response under a verification prompt s . Let $c(y; y^*) \in \{0, 1\}$ denote a task-specific correctness indicator. We define four mutually exclusive outcome categories:

- **Fix:** $c(y_b; y^*) = 0$ and $c(y_p; y^*) = 1$;
- **Break:** $c(y_b; y^*) = 1$ and $c(y_p; y^*) = 0$;
- **Unchanged-correct:** both correct;
- **Unchanged-wrong:** both incorrect.

As a sample-level diagnostic, we define the net correction count $|\text{Fix}| - |\text{Break}|$. This decomposition treats verification prompting as a risk-bearing intervention whose benefit is not guaranteed for any given input.

3.2 Probing Attention Redistribution

To analyze how verification prompting changes internal computation, we extract attention maps from all L layers during the prefill pass before generation begins. For each layer l , we use the final prefill position and compute the following quantities, averaged over heads.

Attention entropy.

$$H^{(l)} = - \sum_{i=1}^n a_i^{(l)} \log a_i^{(l)} \quad (1)$$

where $a_i^{(l)}$ are attention weights over n key positions. Higher entropy indicates a more dispersed attention distribution.

Visual and instruction attention mass. Let \mathcal{V} and \mathcal{I} denote visual-token and instruction-token positions respectively:

$$M_{\text{vis}}^{(l)} = \sum_{i \in \mathcal{V}} a_i^{(l)}, \quad M_{\text{inst}}^{(l)} = \sum_{i \in \mathcal{I}} a_i^{(l)}. \quad (2)$$

A decrease in M_{vis} indicates reduced relative attention to visual tokens; an increase in M_{inst} indicates that instruction tokens absorb a larger share.

To assess whether observed changes are merely due to adding extra text, we compare three conditions: no prompt (baseline), verification prompt, and a neutral prompt that adds non-verification text. Full prompt texts are reported in Appendix A.

3.3 Risk-aware Selective Prompting (RSP)

Since verification prompting can both fix and break predictions, we trigger it selectively. RSP operates as follows:

Signal extraction. For each input, a probe prefill pass (without generation) extracts a scalar uncertainty signal $u(x)$. For LLaVA-1.5, we use layer- l^* attention entropy; for InstructBLIP, we use inverse first-token confidence, $u(x) = 1 - p_{\text{top1}}$, computed from the output logit distribution.

Threshold selection. On a held-out development set, we sweep candidate trigger rates and select threshold τ that maximizes downstream validation performance.

Selective triggering. At inference, the routing rule is $r(x) = \mathbf{1}[u(x) > \tau]$. If triggered, the model answers with the verification prompt; otherwise, it uses the baseline prompt.

RSP is training-free: it requires no parameter updates. A probe prefill is performed for every input; full verification generation is performed only for the triggered subset.

4 Experiments

4.1 Experimental Setup

Models. We evaluate two architecturally distinct LVLMs: (1) **LLaVA-1.5-7B** (Liu et al., 2023), which concatenates 576 image tokens directly into the language model input (Vicuna-7B backbone, 32 layers); and (2) **InstructBLIP-Vicuna-7B** (Dai et al., 2023), which compresses image features into 32 query tokens via a Q-Former module before passing them to a Vicuna-7B language backbone.

Benchmarks. We use **POPE** (Li et al., 2023) for discriminative evaluation, which probes object hallucination through binary yes/no questions at three difficulty levels: *random* ($n=2,910$), *popular* ($n=3,000$), and *adversarial* ($n=3,000$). Images are drawn from MSCOCO 2014 validation. We additionally evaluate on **CHAIR** (Rohrbach et al., 2018) to probe boundaries on open-ended generation; details are reported in Appendix C.

Development and evaluation protocol. We split POPE-random ($n=2,910$) into a development subset ($n_{\text{dev}}=910$) and a disjoint test subset ($n_{\text{test}}=2,000$). The development subset is used for all hyperparameter selection; the test subset and full POPE-popular and POPE-adversarial splits are used only for final evaluation.

For LLaVA-1.5, we select layer-23 attention entropy as the uncertainty signal with threshold $\tau = 1.82$ (top 6% on dev; realized trigger rate 5–7% across test splits). For InstructBLIP, attention entropy is near chance (AUROC ≈ 0.5), likely due to the compressed visual representation from the Q-Former; we use inverse first-token confidence ($1 - p_{\text{top1}}$) as the uncertainty signal, paired with a short cautious prompt (“Be careful.”), yielding realized trigger rates of 10–14% across POPE splits.

Threshold calibration. For each model, the routing threshold τ is selected on the POPE-random development set ($n_{\text{dev}}=910$) and then held fixed for all final evaluations within the same model. We do not claim zero-shot threshold transfer across datasets or architectures; RSP requires a modest calibration set but no gradient-based tuning or auxiliary model training.

Split	Fixes	Breaks	Net	$\Delta\text{Yes}\%$	ΔF1
Random	88	89	−1	−6.4	−0.007
Popular	113	91	+22	−5.4	−0.002
Adversarial	198	92	+106	−8.8	+0.018

Table 1: Fix/break analysis of always-on verification prompting (LLaVA-1.5, POPE, full splits). Breaks remain stable (~ 90) while fixes scale with difficulty. $\Delta\text{Yes}\%$: absolute change in yes-rate (percentage points). ** $p < 0.01$ vs. baseline.

Computational overhead. RSP is training-free but not cost-free: it requires one additional probe prefill pass for each input to extract the uncertainty signal, adding moderate wall-clock overhead. Verification generation is then performed only for the triggered subset of inputs (5–7% for LLaVA-1.5, 10–14% for InstructBLIP). Thus, “training-free” refers to the absence of parameter updates or auxiliary model training, not to zero inference overhead.

Compared methods. (1) *Baseline*: standard inference without verification; (2) *Always-on*: verification prompting applied to all inputs; (3) *RSP*: our proposed selective prompting.

Generation and metrics. All POPE experiments use greedy decoding with `max_new_tokens = 10`. We report F1 (“yes” as positive class), Precision, Recall, and Accuracy. Signal quality is measured by AUROC. Statistical significance is assessed with paired bootstrap resampling ($N = 2,000$, 95% CI).

4.2 Conservative Shift and Difficulty Dependence

We first examine the sample-level effects of always-on verification prompting on LLaVA-1.5. For this diagnostic analysis, we use the full POPE splits to characterize the aggregate effect of always-on prompting; all RSP evaluations follow the held-out protocol described in Section 4.1.

Key finding: asymmetric fix/break pattern.

Table 1 reveals a striking asymmetry: breaks remain roughly constant across splits (89–92), while fixes scale with the number of base errors (88→113→198). On the easiest split, fixes and breaks nearly cancel ($\text{net} = -1$); on the hardest split, fixes far exceed breaks ($\text{net} = +106$, $p < 0.01$). This difficulty dependence is central to our argument: always-on prompting provides little benefit on easy inputs but yields significant improvement on hard inputs.

Layer	ΔH_V %	ΔH_N %	Diff	ΔM_{vis}	M_{inst}
L1	-8.8	-13.3	+4.5	-0.171	0.60
L11	+11.2	+1.2	+10.0	-0.025	0.44
L14	+2.1	-16.6	+18.7	-0.028	0.40
L15	-3.2	-23.0	+19.8	-0.021	0.39
L16	-4.4	-20.5	+16.1	-0.040	0.39
L23	+6.2	+0.7	+5.6	-0.002	0.15
L31	+5.6	+8.4	-2.8	-0.008	0.28

Table 2: Attention changes under verification (V) and neutral (N) prompts relative to baseline (selected layers; full table in Appendix). $\Delta H\%$: change in attention entropy. Diff = $\Delta H_V - \Delta H_N$: difference between verification and neutral controls. M_{inst} : fraction of attention on instruction tokens under verification.

Conservative bias as the underlying mechanism.

Across all splits, verification prompting consistently reduces the yes-rate by 5–9 percentage points and shifts the precision–recall trade-off: Precision increases (e.g., adversarial: 0.747→0.816) while Recall decreases (0.896→0.836). This conservative shift helps when the base model over-hallucinates but provides little benefit when it is already well-calibrated.

4.3 Attention Redistribution Mechanism

To understand *how* verification prompting produces the conservative shift, we extract 32-layer attention maps during prefill on a subset of POPE-random ($n=500$) under three conditions: baseline, verification prompt, and a neutral prompt that adds non-verification text. We report attention entropy $H^{(l)}$, visual attention mass $M_{\text{vis}}^{(l)}$, and instruction attention mass $M_{\text{inst}}^{(l)}$ as defined in Section 3.2.

Finding 1: Instruction tokens absorb attention.

Under verification prompting, instruction tokens attract 38–60% of attention mass in the first 16 layers (Table 2, rightmost column). Visual attention mass decreases in 29 of 32 layers, with the largest drops in early layers (L1: -0.171).

Finding 2: Verification induces a distinct entropy pattern.

The neutral prompt causes middle-layer entropy to *collapse* (L14–17: -17% to -23%), whereas verification prompting maintains or increases entropy in the same layers (L14: +2.1%, L11: +11.2%). The difference column (Diff) highlights verification-specific effects that are not explained by input elongation alone: up to +19.8% at L15.

Interpretation. Together, these results suggest that verification prompting changes the model’s

Split	Baseline	Always-on	RSP	Trig.%
Random	.896	.889	.899	7%
Popular	.864	.862	.865	5%
Adversarial	.810	.827	.812	6%

Table 3: F1 on POPE (LLaVA-1.5). RSP uses L23 attention entropy. On easy/medium inputs, RSP avoids always-on degradation; on adversarial inputs, always-on is more beneficial because the fix/break ratio strongly favors prompting. ** $p < 0.01$.

Split	Baseline	Always-on	RSP	Trig.%
Random	.887	.874	.891	10%
Popular	.839	.842	.852	14%
Adversarial	.818	.818	.826	14%

Table 4: F1 on POPE (InstructBLIP, inverse top-1 confidence, “Be careful.” prompt). RSP numerically improves over baseline on all splits and significantly on popular and adversarial. * $p < 0.05$.

internal computation by reallocating attention toward instruction tokens and maintaining a more dispersed middle-layer attention pattern than a neutral prompt control. The verification condition does not exhibit the entropy collapse seen under neutral prompting, and this pattern aligns with the conservative output shift observed in Section 4.2. These observations suggest that verification prompting is associated with instruction-conditioned attention redistribution, without clear evidence of uniformly improved visual grounding.

4.4 RSP: Selective Intervention

LLaVA-1.5 results. Table 3 shows that RSP remains at or above baseline on all splits (+0.1–0.3% F1) while triggering on only 5–7% of inputs. On random and popular splits, RSP outperforms always-on prompting, demonstrating that selective routing avoids the damage caused by indiscriminate prompting. On adversarial inputs, always-on prompting remains superior (F1 .827 vs. .812 for RSP) because the high base error rate makes the fix/break balance strongly favor prompting (Table 1: 198 fixes vs. 92 breaks). This does not contradict RSP’s motivation: selective routing is most useful in mixed-difficulty settings, where indiscriminate prompting introduces avoidable breaks on easier inputs. In uniformly hard settings, unconditional prompting can be the better choice.

InstructBLIP results. Table 4 shows that RSP with inverse top-1 confidence routing numerically improves over baseline on all three splits (+0.4–

1.3% F1), with significant gains on popular and adversarial, and consistently outperforms always-on prompting. The selection signal must be architecture-aware: middle-layer attention entropy is informative when visual tokens are directly concatenated (LLaVA), whereas output-logit confidence is more reliable when visual information is compressed by a Q-Former (InstructBLIP).

Oracle ceiling and gap analysis. An oracle routing analysis (Appendix B) shows that perfectly selective prompting on only 3–7% of inputs could yield +2.7–5.2% F1, indicating substantial headroom. The gap between RSP and oracle performance likely arises because pre-generation uncertainty captures input-level risk only imperfectly and cannot reliably predict whether prompting will fix or break a specific sample. In addition, RSP uses a hard binary threshold, which may discard borderline cases where adaptive intervention would be preferable. Closing this gap may require generation-aware signals or lightweight learned routers, which we leave to future work.

5 Discussion

RSP currently captures only part of the oracle headroom, indicating room for stronger routing predictors. The current pre-generation signals are validated primarily in discriminative settings and do not directly transfer to open-ended generation, where hallucination may emerge progressively during decoding. Moreover, effective routing signals appear architecture-sensitive, and our experiments are limited to 7B-scale LVLMs.

More broadly, our results suggest that verification prompting should be treated as a risk-bearing intervention rather than a universally beneficial add-on. Practical systems should decide *when* to apply verification prompting, not only *how* to formulate it.

Relationship to decoding-based methods.

Decoding-based hallucination mitigation methods such as VCD (Leng et al., 2024), OPERA (Huang et al., 2024), and DoLa (Chuang et al., 2024) modify the generation procedure through contrastive decoding, attention penalties, or layer-wise logit contrasting. RSP addresses a different question: given a prompt-based verification intervention, *when* should it be applied? It is therefore orthogonal to decoding-time interventions and could in principle be combined with them. Our goal is

not to replace these methods, but to characterize the risk of uniform prompting and provide a training-free selective routing mechanism. A full combination study is beyond the scope of this work.

6 Conclusion

We showed that verification prompting in LVLMs is a risk-bearing intervention: the errors it corrects increase with input difficulty, while the errors it introduces persist across difficulty levels. This explains why always-on prompting helps on hard inputs but offers little benefit—and can harm—easier ones. Our probing analysis shows that this conservative shift is associated with attention redistribution from visual tokens toward instruction tokens. Based on these findings, we proposed RSP, a training-free selective prompting method that uses pre-generation uncertainty to trigger verification selectively, mitigating the degradation of indiscriminate prompting while remaining close to or above baseline performance. Our cross-architecture results further show that effective routing signals vary across the architectures we study, motivating future work on stronger and more general predictors.

Limitations

Our work has several limitations. First, our main experiments are conducted on two open-source LVLMs, LLaVA-1.5 and InstructBLIP. Although they represent different visual-token interfaces, broader validation on additional architectures, model scales, and closed-source systems such as GPT-4V or Gemini remains future work. In particular, some closed-source models may not expose the internal attention or logit signals required by RSP.

Second, RSP requires a small development set to select the routing threshold τ . The optimal threshold may vary across models, datasets, and task domains, and we do not study zero-shot threshold transfer or adaptive threshold selection.

Third, RSP is training-free but not inference-free. It requires one probe prefill pass for each input to extract the uncertainty signal, introducing additional inference overhead even though verification generation is used only for the triggered subset.

Fourth, our attention analysis is observational. While we find that verification prompting is associated with attention redistribution from visual tokens toward instruction tokens, this does not establish

a causal mechanism or fully explain the model’s internal decision process.

Finally, our evaluation focuses primarily on English object-hallucination settings. Our CHAIR analysis suggests that current pre-generation signals may not directly transfer to open-ended generation, and multilingual or cross-lingual multimodal settings remain unexplored.

References

- Chao Chen, Kai Liu, Ze Chen, Yi Gu, Yue Wu, Mingyuan Tao, Zhihang Fu, and Jieping Ye. 2024. INSIDE: LLMs’ internal states retain the power of hallucination detection. In *International Conference on Learning Representations (ICLR)*.
- Yu-Neng Chuang, Leisheng Yu, Guanchu Wang, Lizhe Zhang, and 1 others. 2025. Confident or seek stronger: Exploring uncertainty-based on-device LLM routing from benchmarking to generalization. In *Advances in Neural Information Processing Systems (NeurIPS)*. ArXiv:2502.04428.
- Yung-Sung Chuang, Yujia Xie, Hongyin Luo, Yoon Kim, James Glass, and Pengcheng He. 2024. DoLa: Decoding by contrasting layers improves factuality in large language models. In *International Conference on Learning Representations (ICLR)*.
- Wenliang Dai, Junnan Li, Dongxu Li, Anthony Meng Huat Tiong, Junqi Zhao, Weisheng Wang, Boyang Li, Pascale Fung, and Steven Hoi. 2023. InstructBLIP: Towards general-purpose vision-language models with instruction tuning. In *Advances in Neural Information Processing Systems (NeurIPS)*.
- Jingyuan Deng and Yujia Yang. 2025. MaskCD: Mitigating LVLM hallucinations by image head masked contrastive decoding. In *Findings of the Association for Computational Linguistics: EMNLP 2025*.
- Shehzaad Dhuliawala, Mojtaba Komeili, Jing Xu, Roberta Raber, Xian Li, Adina De Melo, and Mike Stanton. 2023. Chain-of-verification reduces hallucination in large language models. *arXiv preprint arXiv:2309.11495*.
- Qidong Huang, Xiaoyi Dong, Pan Zhang, Bin Wang, Conghui He, Jiaqi Wang, Dahua Lin, Weiming Zhang, and Nenghai Yu. 2024. OPERA: Alleviating hallucination in multi-modal large language models via over-trust penalty and retrospection-allocation. In *Proceedings of the IEEE/CVF Conference on Computer Vision and Pattern Recognition (CVPR)*.
- Ziwei Ji, Delong Chen, Etsuko Ishii, Samuel Cahyawijaya, Yejin Bang, Bryan Wilie, and Pascale Fung. 2024. LLM internal states reveal hallucination risk faced with a query. In *Proceedings of the 7th BlackboxNLP Workshop*.
- Hazel Kim, Tom A. Lamb, Adel Bibi, Philip Torr, and Yarin Gal. 2025. Detecting LLM hallucination through layer-wise information deficiency: Analysis of ambiguous prompts and unanswerable questions. In *Proceedings of the 2025 Conference on Empirical Methods in Natural Language Processing (EMNLP)*, pages 32310–32322, Suzhou, China. Association for Computational Linguistics.
- Jannik Kossen, Jiatong Han, Lisa Schut, and Yarin Gal. 2024. Semantic entropy probes: Robust and cheap hallucination detection in LLMs. *arXiv preprint arXiv:2406.15927*. ICML 2024 Workshop on Foundation Models in the Wild.
- Lorenz Kuhn, Yarin Gal, and Sebastian Farquhar. 2023. Semantic uncertainty: Linguistic invariances for uncertainty estimation in natural language generation. In *International Conference on Learning Representations (ICLR)*. Spotlight.
- Sicong Leng, Hang Zhang, Guanzheng Chen, Xin Li, Shijian Lu, Chunyan Miao, and Lidong Bing. 2024. Mitigating object hallucinations in large vision-language models through visual contrastive decoding. In *Proceedings of the IEEE/CVF Conference on Computer Vision and Pattern Recognition (CVPR)*.
- Yifan Li, Yifan Du, Kun Zhou, Jinpeng Wang, Wayne Xin Zhao, and Ji-Rong Wen. 2023. Evaluating object hallucination in large vision-language models. In *Proceedings of the 2023 Conference on Empirical Methods in Natural Language Processing (EMNLP)*.
- Haotian Liu, Chunyuan Li, Qingyang Wu, and Yong Jae Lee. 2023. Visual instruction tuning. In *Advances in Neural Information Processing Systems (NeurIPS)*. Oral.
- Aman Madaan, Niket Tandon, Prakhar Gupta, Skyler Hallinan, Luyu Gao, Sarah Wiegrefe, Uri Alon, Nouha Dziri, Shrimai Prabhumoye, Yiming Yang, and 1 others. 2023. Self-refine: Iterative refinement with self-feedback. In *Advances in Neural Information Processing Systems (NeurIPS)*.
- Alexander Nikitin, Jannik Kossen, Yarin Gal, and Pekka Marttinen. 2024. Kernel language entropy: Fine-grained uncertainty quantification for LLMs from semantic similarities. In *Advances in Neural Information Processing Systems (NeurIPS)*.
- OpenAI. 2023. GPT-4V(ision) system card. <https://openai.com/research/gpt-4v-system-card>.
- Anna Rohrbach, Lisa Anne Hendricks, Kaylee Burns, Trevor Darrell, and Kate Saenko. 2018. Object hallucination in image captioning. In *Proceedings of the 2018 Conference on Empirical Methods in Natural Language Processing (EMNLP)*.
- Zayne Sprague, Fangcong Yin, Juan Diego Rodriguez, Dongwei Jiang, Manya Wadhwa, Prasann Singhal,

Xinyu Zhao, Xi Ye, Kyle Mahowald, and Greg Durrett. 2024. Mind your step (by step): Chain-of-thought can reduce performance on tasks where thinking makes humans worse. *arXiv preprint arXiv:2410.21333*.

Ghosh Sreyan, Srikanth Chandra, Nithin Evuru, and 1 others. 2025. Visual description grounding reduces hallucinations and boosts reasoning in LVLMs. In *International Conference on Learning Representations (ICLR)*.

Zifu Wan, Ce Zhang, Silong Yong, Martin Q. Ma, Simon Stepputtis, Louis-Philippe Morency, Deva Ramanan, Katia Sycara, and Yaqi Xie. 2025. ONLY: One-layer intervention sufficiently mitigates hallucinations in large vision-language models. *arXiv preprint arXiv:2507.00898*.

Le Yang, Ziwei Zheng, Boxu Chen, Zhengyu Zhao, Chenhao Lin, and Chao Shen. 2025. Nullu: Mitigating object hallucinations in large vision-language models via HalluSpace projection. In *IEEE/CVF Conference on Computer Vision and Pattern Recognition (CVPR)*.

Shukang Yin, Chaoyou Fu, Sirui Zhao, Tong Xu, Hao Wang, Dianbo Sui, Yunhang Shen, Ke Li, Xing Sun, and Enhong Chen. 2024. Woodpecker: Hallucination correction for multimodal large language models. *Science China Information Sciences*, 67:220105.

Ce Zhang, Zifu Wan, Zhehan Kan, Martin Q. Ma, Simon Stepputtis, Louis-Philippe Morency, Deva Ramanan, Katia Sycara, and Yaqi Xie. 2025. Self-correcting decoding with generative feedback for mitigating hallucinations in large vision-language models. In *International Conference on Learning Representations (ICLR)*.

Xiaofeng Zhang, Yihao Quan, Chaochen Gu, Chaochen Shen, Xiaosong Yuan, Shaotian Yan, Hao Cheng, Kaijie Wu, and Jieping Ye. 2024. Seeing clearly by layer two: Enhancing attention heads to alleviate hallucination in LVLMs. *arXiv preprint arXiv:2411.09968*.

Yiyang Zhou, Chenhang Cui, Jaehong Yoon, Linjun Zhang, Zhun Deng, Chelsea Finn, Mohit Bansal, and Huaxiu Yao. 2024. Analyzing and mitigating object hallucination in large vision-language models. In *International Conference on Learning Representations (ICLR)*.

A Prompt Texts

LLaVA-1.5 Verification Prompt.

You are a precise visual content describer. Before answering, briefly verify in your mind: Can I ACTUALLY see this object in the image? Only answer yes if the object is clearly visible. Do not guess or infer objects that are not clearly present.

LLaVA-1.5 Neutral Prompt.

You are a precise visual content describer. RULES: 1) Only describe objects, attributes, and relationships that are ACTUALLY VISIBLE in the image. 2) If you are unsure whether something exists in the image, DO NOT mention it. 3) Do not use your prior knowledge to infer objects that are not clearly visible. 4) Use hedging language (e.g., ‘appears to be’, ‘likely’) for anything uncertain.

InstructBLIP Cautious Prompt.

Be careful.

B Oracle Routing Ceiling

Split	Baseline	Oracle	$\Delta F1$	Prompt%
Random	.896	.924	+0.028	3.0%
Popular	.864	.897	+0.033	3.8%
Adversarial	.810	.862	+0.052	6.6%

Table 5: Oracle routing ceiling for LLaVA-1.5. Perfect routing would prompt only 3–7% of inputs while yielding substantially larger F1 gains, indicating headroom for stronger routing signals.

C CHAIR Boundary Analysis

Pre-generation uncertainty signals are near chance for predicting CHAIR hallucination (prefill entropy AUROC = 0.44), while generation-time mean entropy provides a moderate signal (AUROC = 0.63). This contrast suggests that, for open-ended generation, useful uncertainty information emerges during decoding rather than being reliably available before generation begins, representing a boundary of the current pre-generation routing formulation.

D Full Layer-wise Analysis

Table 6 reports the AUROC of each layer’s attention entropy for predicting whether verification prompting will change the model’s answer (pilot study, $n = 100$).

Why Layer 23 over Layer 30. In the pilot study ($n = 100$), Layer 30 achieves the highest AUROC (.675 vs. .643 for Layer 23). However, a larger validation ($n = 489$) reveals that Layer 30’s AUROC drops to .298—below chance and inverted in polarity—while Layer 23’s AUROC increases to .796 (Table 7). This instability is also reflected in downstream RSP performance: Layer 30 requires a 50% trigger rate to achieve its best F1 of .896,

Layer	AUROC	$\Delta H\%$	Layer	AUROC
0	.578	-1.8	16	.526
1	.528	-2.2	17	.524
2	.583	+16.7	18	.554
3	.557	+5.1	19	.504
4	.580	-8.4	20	.559
5	.546	+2.1	21	.526
6	.581	+2.9	22	.616
7	.536	+11.4	23	.643
8	.521	+9.2	24	.619
9	.619	+11.4	25	.558
10	.509	+25.9	26	.549
11	.503	+7.3	27	.578
12	.549	+13.6	28	.575
13	.529	+19.9	29	.501
14	.589	+28.1	30	.675
15	.631	+27.2	31	.516

Table 6: Layer-wise AUROC and entropy change under verification prompting (LLaVA-1.5, pilot $n = 100$). $\Delta H\%$: percentage change in attention entropy relative to baseline. Layer 23 is selected on the development set; its full-scale AUROC is 0.60 (random), 0.67 (popular/adversarial).

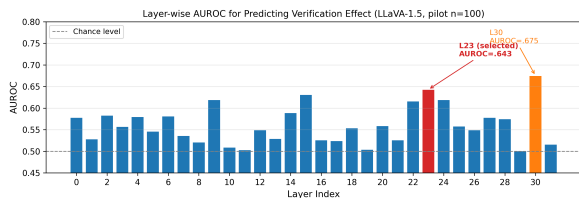


Figure 1: Layer-wise AUROC for predicting whether verification prompting will change the model’s answer (LLaVA-1.5, pilot $n = 100$). Layer 23 (red) is selected; Layer 30 (orange) achieves higher pilot AUROC but is unstable at larger sample sizes (Table 7).

whereas Layer 23 achieves $F1 = .900$ at only 10% trigger rate. We therefore select Layer 23 for its stability and efficiency.

E Trigger Rate Sensitivity

Sensitivity to trigger rate. Table 8 reports RSP performance as the routing threshold is varied across POPE splits. On random and popular splits, performance peaks at 5–7% trigger rate and degrades as the rate increases toward always-on, confirming that selective routing at a low trigger rate is beneficial for easy and medium inputs. On adversarial inputs, performance increases monotonically with trigger rate, consistent with the finding that the fix/break ratio strongly favors prompting in high-difficulty settings (Section 4.2).

Layer	Pilot AUROC ($n = 100$)	Val. AUROC ($n = 489$)	Best RSP F1	Trigger%
15	.631	.677	.902	30%
23	.643	.796	.900	10%
30	.675	.298	.896	50%
31	.516	.317	.899	50%

Table 7: Layer comparison for RSP routing signal (LLaVA-1.5, POPE-random). Layer 23 has the highest validation AUROC and achieves competitive F1 at the lowest trigger rate. Layers 30 and 31 show AUROC inversion at larger sample sizes.

Trigger rate	Random	Popular	Adversarial
Baseline (0%)	.896	.864	.810
3%	.898	.865	.810
5%	.898	.864	.810
7% [†]	.899	.865	.812
10%	.898	.865	.812
15%	.896	.864	.811
20%	.895	.863	.811
50%	.896	.865	.822
Always-on (100%)	.889	.862	.827

Table 8: RSP F1 across trigger rates (LLaVA-1.5, L23 attention entropy, full POPE splits). [†] = threshold used in main experiments. On random and popular splits, low trigger rates outperform always-on; on adversarial, performance increases monotonically with trigger rate.